Gondwana Research, V. 5, No. 4, pp. 823-835.

ISSN: 1342-937X

GR Gondwana Research

Granulite Facies Relics in the Early Paleozoic Kyanite-bearing Ultrabasic Metacumulate in the Oeyama Belt, the Inner Zone of Southwestern Japan

Tatsuki Tsujimori [1*] and Akira Ishiwatari [2]

[1] *Research Institute of Natural Sciences, Okayama University of Science, Okayama 700-0005, Japan, E-mail: tatsukix@rins.ous.ac.jp*

[2] *Department of Earth Sciences, Faculty of Science, Kanazawa University, Kanazawa 920-1192, Japan*

**Corresponding author*

(Manuscript received July 25, 2001; accepted May 9, 2002)

Abstract

Granulite facies relics are found in the early Paleozoic kyanite-bearing melanocratic metagabbro from the Fuko Pass metacumulate mass of the Oeyama belt, southwestern Japan. The granulite facies assemblage consists of relict Al-rich clinopyroxene (up to 8.5 wt.% Al_2O_3) and pseudomorphs of spinel and plagioclase. The spinel pseudomorphs consist mainly of symplectic intergrowth of corundum and magnetite with minor gahnitic spinel. The plagioclase pseudomorphs are composed mainly of clinozoisite with minor kyanite. The symplectite suggests oxidation and Mg-depletion of the original spinel: hercynite ($3FeAl_2O_4$)+(O) = corundum ($3Al_2O_3$)+magnetite (Fe_3O_4). This oxidation reaction may have taken place at 700–900°C temperature. The melanocratic metagabbro has later been hydrated to form the epidote amphibolite assemblage represented by clinozoisite+kyanite+paragonite. The clinozoisite+kyanite assemblage has further reacted to form margarite at a lower temperature. The first granulite facies assemblage implies that the metacumulate has originally constituted a basal part of thick oceanic crust, and then has experienced the high-P/T type metamorphism in a subduction zone. This indicates that the thick oceanic crust has been formed and accreted to the Circum-Pacific orogenic belt in the early Paleozoic time.

Key words: Lower crustal granulite, Al-rich clinopyroxene, corundum-magnetite intergrowth, Fuko Pass metacumulate, Oeyama belt.

Introduction

The lower crustal basic to ultrabasic granulites occur at the basal cumulate section from some Circum-Pacific ophiolites (e.g., Yakuno, SW Japan: Ishiwatari, 1985; Tonsina, Alaska: DeBari and Coleman, 1989; Bikin, Eastern Russia: Vysotskiy, 1994). These ophiolitic granulites commonly bear the two pyroxenes+plagioclase +Al spinel assemblage instead of the olivine+plagioclase assemblage. Ishiwatari (1985a) proposed that the lower crustal granulite of ophiolite represents the unusually thick oceanic crust, which is about three to five times the average thickness of modern oceanic crust (7.1 km; White et al., 1992). In the modern oceanic lithosphere, the thick oceanic crust is found beneath the huge oceanic plateaus, such as the Ontong Java, Kerguelen, and Caribbean plateaus (e.g., Saunders et al., 1996). The medium-pressure granulite facies condition (around 1.0 GPa) is attained at the Moho level beneath the thick oceanic crust. In fact, the xenoliths of lower crustal basic to ultrabasic granulites captured by basaltic lava have been reported from the Kerguelen Plateau (Grégoire et al., 1994, 1998). However, granulite facies spinel metagabbro is also reported as xenoliths in island-arc volcanoes such as in Alaska and Japan (Francis, 1976; Takahashi, 1978), and DeBari and Coleman (1989) proposed an island-arc origin for their mafic-ultramafic rocks. In any case, the granulite facies metagabbros in Circum-Pacific ophiolitic belts give an evidence of the accretion of the thick oceanic crust during oceanward growth of the orogenic belts.

The Oeyama belt in the Inner Zone of SW Japan is one of the oldest ophiolitic belts in the Circum-Pacific orogenic belt. The Fuko Pass metacumulate mass of Siluro–

Ordovician hornblende K–Ar age occurs as a tectonic block in the easternmost (Oeyama) body of the Oeyama belt (Tsujimori, 1999; Tsujimori et al., 2000). Although the Fuko Pass metacumulate rocks consist mainly of epidote amphibolite facies minerals, we report here on petrographic and mineral-chemical evidences for the preceding granulite facies assemblage and discuss their metamorphic evolution.

Geologic Outline

In the Inner Zone of SW Japan, several ultramafic bodies are exposed in the Chugoku Mountains (Arai, 1980). Kurokawa (1985) first reported that the easternmost Oeyama body is a dismembered ophiolite complex composed of residual peridotite and cumulate rocks. Ishiwatari (1991) grouped these ultramafic bodies into 'Oeyama ophiolite', because they are different in petrologic nature (absence of igneous layering, common occurrence of graphic chromian spinel, etc.) and hornblende K–Ar age (early Paleozoic; Nishimura and Shibata, 1989) from the nearby late Paleozoic Yakuno ophiolite. This grouping is generally accepted as the 'Oeyama belt' in recent geotectonic considerations (e.g., Isozaki, 1996; Maruyama, 1997). The ultramafic bodies of the Oeyama belt occupy the highest position structurally, and many of them rest on the late Paleozoic blueschist of the Renge belt (e.g., Tsujimori and Itaya, 1999). The ultramafic bodies are composed mainly of serpentinized harzburgite (more lherzolitic in eastern bodies) and dunite with minor podiform chromitite and mafic intrusions (e.g., Arai, 1980; Kurokawa, 1985; Matsumoto et al., 1997). Hayasaka et al. (1995) reported the Sm–Nd ages of about 560 Ma for the gabbroic intrusions, suggesting Cambrian igneous age. The bodies were partly overprinted by contact metamorphism of Cretaceous granitic intrusions (e.g., Arai, 1975), though primary minerals are partly preserved.

The simplified geologic map of the Oeyama area is shown in figure 1. The Oeyama peridotite body tectonically

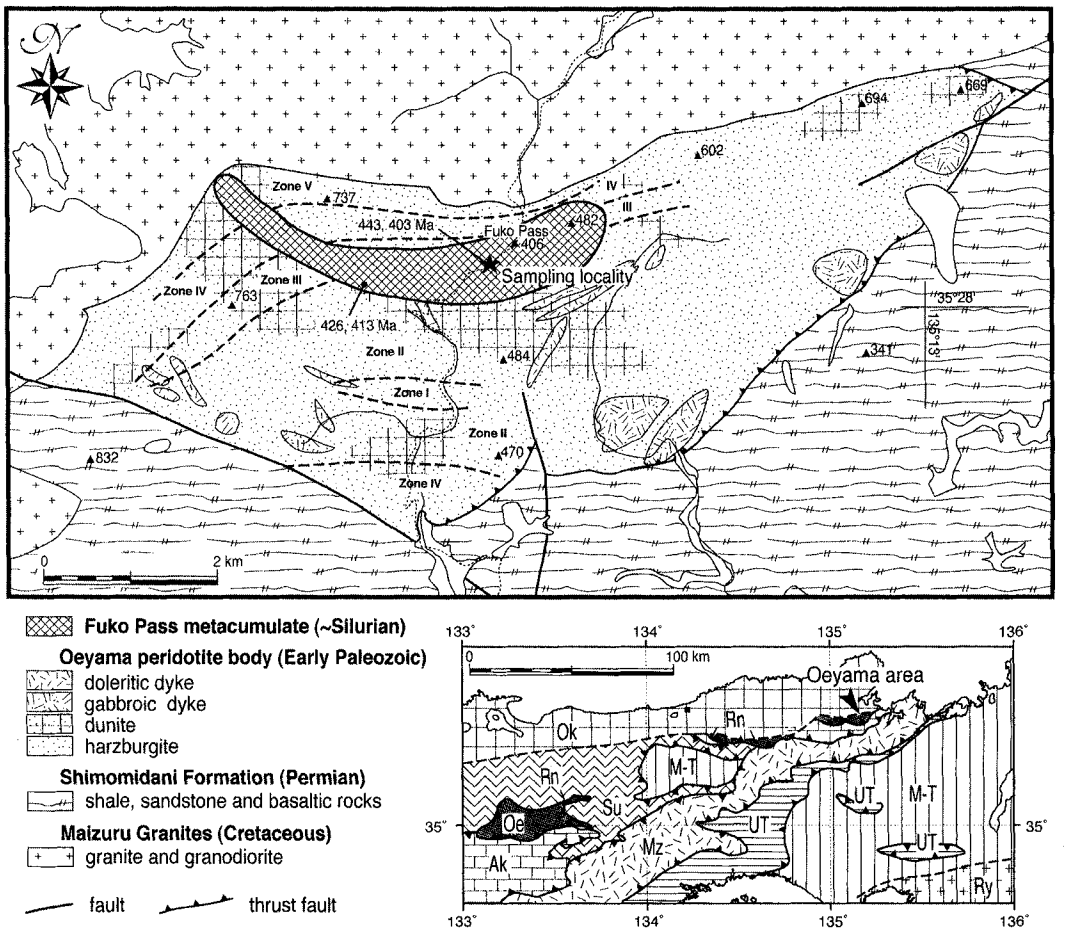

Fig. 1. Geologic map of the Oeyama area. Lithologic distribution and classification of residual peridotite is based on Uda (1984). Distribution of the Fuko Pass metacumulate and other rocks is based on Kurokawa (1985). Broken lines represent the boundary between Uda (1984)'s metamorphic zones of the contact aureole. Ok = Oki belt, Oe = Oeyama belt, Rn = Renge belt, Mz = Maizuru belt, UT = Ultra-Tamba belt, M-T = Mino-Tamba belt, Ry = Ryoke belt.

overlies the Permian accretionary complex of the Akiyoshi belt on the south (Shimomidani Formation: Ishiga and Suzuki, 1988). In this area, the peridotite is mostly composed of harzburgite, which are cut by doleritic or gabbroic dykes (Uda, 1984; Kurokawa, 1985). The Fuko Pass metacumulate mass (4.5 × 1.5 km) occupies the topographically higher portion of the Oeyama peridotite body (10 × 3 km) (Fig. 1). The epidote amphibolite facies mineral assemblage is ubiquitous in the Fuko Pass mass, but is absent in the gabbroic intrusions. Thus, we interpret that the Fuko Pass mass is tectonically juxtaposed with (possibly overlying) the Oeyama peridotite body. The protoliths of the Fuko Pass mass are basic and ultrabasic cumulates (Kuroda et al., 1976; Kurokawa, 1985; Tsujimori, 1999). The foliated epidote amphibolite of the Fuko Pass mass contains a critical high-pressure mineral assemblage: hornblende+clinozoisite+kyanite +paragonite+rutile+albite (Tsujimori, 1999). Staurolite, corundum and secondary margarite were also described from the mass (Kurokawa, 1975; Tsujimori, 1999). Hornblende K–Ar ages of the foliated epidote amphibolite yield 443–403 Ma (Tsujimori et al., 2000). The Oeyama peridotite body has been highly serpentinized, and has later been overprinted by contact metamorphism of the Cretaceous granitic intrusions. Uda (1984) divided the Oeyama ultramafic body into five contact metamorphic zones: (I) antigorite, (II) olivine+antigorite+diopside, (III) olivine+antigorite+tremolite, (IV) olivine+talc± tremolite± magnesio-cummingtonite+tremolite, (V) olivine+enstatite± tremolite± hornblende, and the Fuko Pass metacumulate mass extends from Zone II to Zone V.

Occurrence and Bulk Rock Chemistry

The studied mafic and ultramafic metacumulate rocks were sampled at a weathered outcrop (20 × 3 m) near the Fuko Pass, which is described in detail by Kurokawa (1985). The outcrop is located in the Zone II of Uda (1984) (Fig. 1), but the effect of contact metamorphism is exceptionally scarce in the outcrop. In this outcrop, the massive coarse-grained metagabbro, virtually undeformed, occurs as irregular blocks in the matrix of foliated (or gneissose) epidote amphibolite. Tsujimori (1999) used the term of 'metagabbro' to indicate any undeformed epidote amphibolite in which original gabbroic texture was well-preserved, and distinguished it from the 'foliated epidote amphibolite'. The metagabbro is subdivided into leucocratic and melanocratic varieties by the content of clinozoisite. The bulk rock major and trace compositions of the two metagabbro varieties and foliated epidote amphibolite suggest that their protoliths are highly fractionated troctolitic cumulate with abundant anorthite-rich plagioclase (Tsujimori, 1999). The relict granulite facies assemblage is found only in the melanocratic metagabbro. The melanocratic metagabbro is ultrabasic (38.9–39.0 wt.% SiO_2), and is characterized by high Al_2O_3 (18.9–19.4 wt.%), high CaO (13.1–14.3 wt.%), Fe_2O_3* (11.8–12.3 wt.%), MgO (11.2–11.4 wt.%), and low Na_2O (0.8–0.9 wt.%) (Table 1).

Table 1. Bulk-rock composition of the melanocratic metagabbro (samples SPMG01 and SPMG02). For comparison, the foliated epidote amphibolite (sample EA01) is also listed.

Sample	SPMG01	SPMG02	EA01
Major-element compositions (in weight %)			
SiO_2	38.86	39.04	41.08
TiO_2	0.56	0.52	0.78
Al_2O_3	19.41	18.92	20.63
Fe_2O_3*	12.31	11.75	12.78
MnO	0.10	0.10	0.16
MgO	11.37	11.19	6.74
CaO	13.09	14.28	14.08
Na_2O	0.88	0.82	1.84
K_2O	0.14	0.11	0.36
P_2O_5	0.01	0.01	0.05
Total	96.73	96.74	98.5
Trace-element compositions (in ppm)			
Sc	143.1	135.5	43.3
Cr	64.0	52.3	32.5
Co	74.4	77.5	60.7
Ni	97	99	18
Cu	109	105	123
Zn	224	166	92
Rb	n.d.	n.d.	6
Sr	147	139	402
Y	12	11	20
V	633	610	536
Zr	21	22	25
Ba	144	117	156
La	0.9	1.2	1.5
Sm	1.3	1.3	2.2
Eu	0.5	0.6	0.9
Lu	0.2	n.d.	0.3
Th	4	n.d.	1

* Total Fe as Fe_2O_3.

Petrography

The melanocratic metagabbro is coarse-grained (5–15 mm), undeformed ultrabasic rock. It consists mainly of Ca-amphibole, clinopyroxene, corundum-magnetite symplectite, chlorite and clinozoisite, with small amount of kyanite, margarite, rutile and paragonite. Clinopyroxene and corundum-magnetite symplectite are partly replaced by later hydrous minerals. Relict clinopyroxene appears either as equigranular grains (3–6 mm in diameter) partly replaced by Ca-amphibole (Fig. 2a, 2b) or as small irregular crystals (<0.5 mm) that are enclosed in Ca-amphibole (Fig. 2c). The euhedral

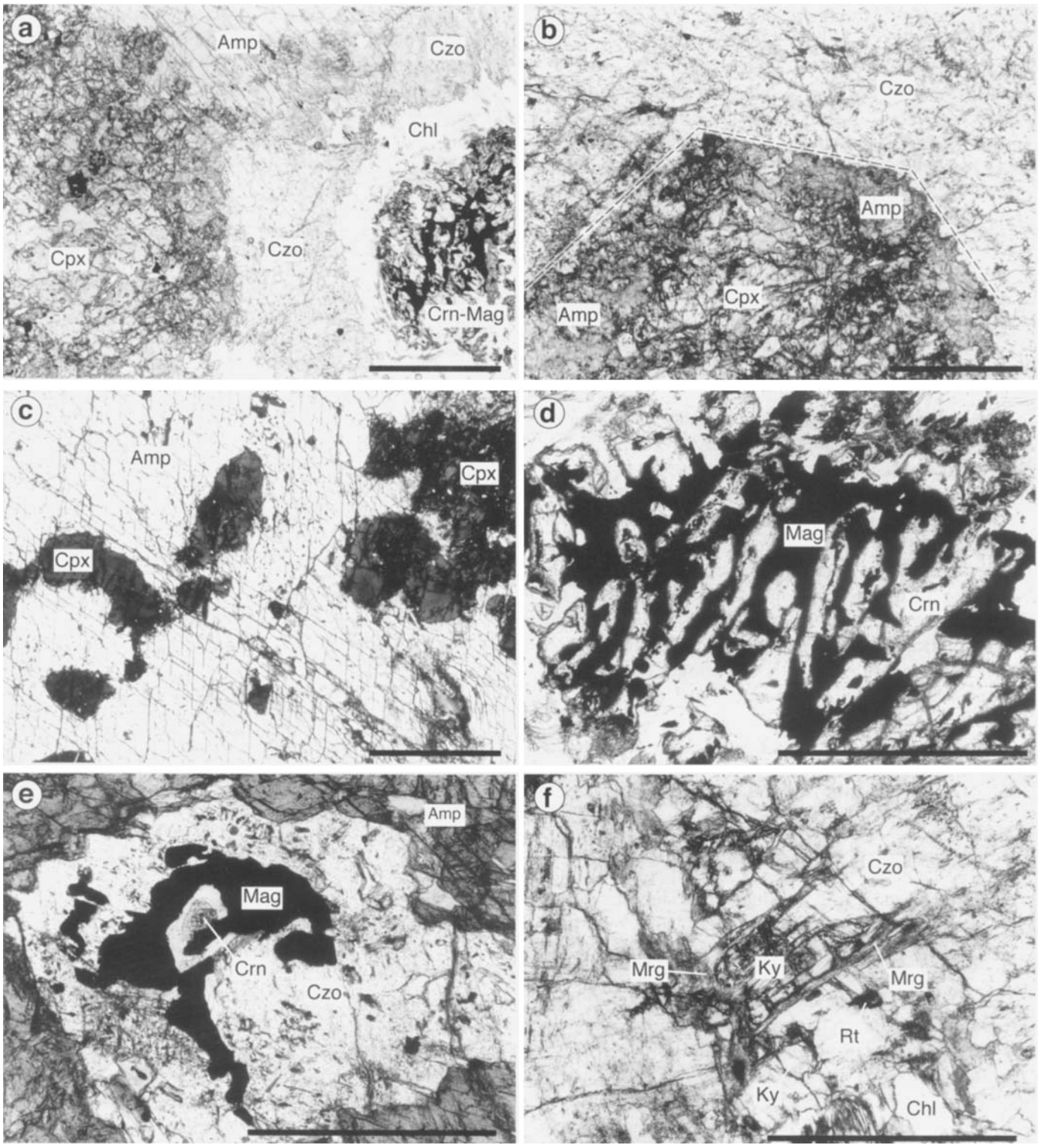

Fig. 2. Photomicrographs showing textural relationship of minerals in the melanocratic metagabbro from the Fuko Pass mass. (a) Granulite facies relics (clinopyroxene and corundum-magnetite symplectite) in the melanocratic metagabbro. (b) Clinopyroxene replaced by Ca-amphiboles at the rim. The original crystal faces remain at the boundary of clinozoisite-rich domain. (c) Ca-amphibole replacing relict clinopyroxene. Relict clinopyroxene shows same extinction position. (d) Symplectitic intergrowth of corundum and magnetite in the spinel pseudomorph. Minor amount of gahnitic spinel and sometimes ilmenite are found in the symplectite. (e) Graphic magnetite with tiny corundum surrounded by clinozoisite. (f) Kyanite and rutile included in the clinozoisite-rich domain. Secondary margarite is developed at the boundary between kyanite and clinozoisite. The scale bars are 1.0 mm for (a), (b) and (c), and 0.5 mm for (d), (e) and (f). All photomicrographs are plane polarized light, except for (c) that is crossed polarized light. Abbreviations: Amp = Ca-amphibole, Chl = chlorite, Crn = corundum, Czo = clinozoisite, Cpx = clinopyroxene, Ky = kyanite, Mag = magnetite, Mrg = margarite.

crystal surface of clinopyroxene is rarely preserved where the mineral is in contact with the clinozoisite-rich domain (Fig. 2b). The corundum-magnetite symplectite consists mainly of intergrowth of corundum and graphic magnetite with minor amounts of gahnitic spinel. Ilmenite is sometimes associated with the symplectite. The symplectite is equi-dimensional in its outer shape (about 1–5 mm in diameter, usually 2–3 mm) (Fig. 2a). The shape and mineral assemblage indicates that the symplectite is a pseudomorph after hercynitic spinel. The corundum-magnetite symplectite is always corroded by hydrous corona consisting mainly of clinozoisite and chlorite. In some cases, corundum in the symplectite was consumed to produce clinozoisite, and only magnetite remained (Fig. 2e). In rare cases, margarite replaces corundum in the corundum-magnetite symplectite. Ca-amphibole occurs as replacements of relic clinopyroxene, inclusions within clinozoisite-rich domain, and discrete crystals. Minute exsolved magnetite grains (<0.03 mm in length) sometimes occur along cleavages. Mosaic aggregates of clinozoisite form the clinozoisite-rich domain in the rock. The clinozoisite-rich domain is irregular in shape (2–15 mm in size) and fills interstices between clinopyroxene and symplectite. Coexisting clinozoisite and zoisite are sometimes found in the domain. Prismatic kyanite (<0.5 mm), chlorite (<1.5 mm), rutile (<0.2 mm) and sometimes paragonite (<0.05 mm) are also present within clinozoisite domains (Fig. 2f). Kyanite within clinozoisite-rich domains is usually replaced by margarite. Chlorite occurs as aggregates in the hydrous corona surrounding the corundum-magnetite symplectite. It also forms chlorite-rich clot (3–5 mm in size). The randomly-oriented prismatic epidote (<1 mm in length) and tiny magnetite are frequently associated with the chlorite clot.

Mineral Chemistry

Analytical techniques

Electron microprobe analysis was carried out with JEOL JXA-8800R at Kanazawa University and JEOL JXA-8900R at Okayama University of Science. The quantitative analyses for rock-forming minerals were performed with 15 kV accelerating voltage, 12 nA beam current and 3 μm beam size. Natural and synthetic silicate and oxides were used for calibration. The ZAF method was employed for matrix corrections. Selected analyses of granulite facies relics and hydrous minerals are presented in table 2.

Clinopyroxene

Relict clinopyroxene contains high Al (up to 8.5 wt.% Al_2O_3) (Fig. 3a), high Ti (up to 0.88 wt.% TiO_2) and low Na (less than 0.34 wt.% Na_2O). The X_{Mg} varies between 0.78 to 0.94, and shows negative correlation with Al (Fig. 3b) and Ti contents. The Al content is depleted gradually toward the contact with clinozoisite.

Spinel pseudomorph (corundum-magnetite symplectite)

Corundum in the spinel pseudomorph contains 0.6–1.7 wt.% Fe_2O_3 and less than 0.1 wt.% Cr_2O_3. Magnetite intergrowing with corundum contains 0.2–1.4 wt.% Al_2O_3 and 0.2–0.4 wt.% TiO_2. Gahnitic spinel often shows exsolution texture, in which Ti-rich spinel lamellae (0.5–6.0 wt.% TiO_2) are developed parallel to the {100} plane of Ti-poor spinel (less than 0.2 wt.% TiO_2), which is characterized by higher Zn content (10–21 wt.% ZnO) and higher X_{Mg} (0.43–0.92) than the Ti-rich gahnitic spinel (7–14 wt.% ZnO and X_{Mg} = 0.24–0.51) (Figs. 4a and 4b). Ilmenite in the corundum-magnetite symplectite contains significant amounts of Mn (2–7 wt.% MnO), and the Fe^{2+}/Mn ratio varies from 5 to 19. The average of $Ti/(Ti+Fe^{3+})$ ratio is 0.94.

Ca-amphiboles

Ca-amphiboles in melanocratic metagabbro have mainly tschermakitic and pargasitic compositions, containing up to 16.3 wt.% Al_2O_3 and 1.2 wt.% TiO_2. However, they vary considerably in the Si content (6.0–7.8 p.f.u. for O = 23) (Fig. 5a). Ca-amphiboles with actinolitic or tremolitic compositions are identified at the rim of relatively coarse-grained crystals. The overall X_{Mg} of Ca-amphiboles in the melanocratic metagabbro ranges from 0.73 to 0.93. The Na on the B-site (Na_B) of Ca-amphiboles in metagabbro is significantly lower than that in the foliated epidote amphibolite of the same outcrop (Fig. 5b), apparently due to different bulk rock composition.

Epidote group minerals

In the clinozoisite-rich domain, clinozoisite has moderate Y_{Fe} (= $Fe^{3+}/(Fe^{3+}+Al)$) (0.12–0.17), and it sometimes coexists with zoisite (Y_{Fe} = 0.04–0.07). Coronitic clinozoisite surrounding the spinel pseudomorph has moderate Y_{Fe} (0.10–0.16). The Y_{Fe} is significantly high (Y_{Fe} = 0.21–0.23) at the higher birefringence part in the clinozoisite-rich domain. On the other hand, prismatic epidote coexists with secondary chlorite high Y_{Fe} (0.26–0.30).

Other minerals

Kyanite contains a trace of Fe_2O_3 (about 0.7 wt.%). Margarite formed along the contact between kyanite and clinozoisite has higher paragonite component (Na/(Na+Ca) = 0.16–19) than those replacing corundum (Na/(Na+Ca) <0.10). Chlorite in hydrous corona around

Table 2. Representative EPMA analyses of rock-forming minerals of melanocratic metagabbro.

	Clinopyroxene				Spinel pseudomorph			Czo-rich domain					Ca-amp		Later stage		
Wt.%					Crn	Mag	Zn-Sp	Czo	(Zo-Czo pair)		Ky	Pg	(replacing Cpx)		Mrg	Ep	Chl
SiO_2	47.72	48.62	49.45	53.30	0.06	0.03	0.04	38.39	37.48	38.58	37.69	45.84	42.95	43.58	31.30	38.25	29.49
TiO_2	0.70	0.76	0.73	0.41	0.10	0.29	0.13	0.14	0.12	0.11	0.00	0.08	1.11	0.63	0.04	0.21	0.00
Al_2O_3	8.31	7.36	6.83	1.95	98.53	1.00	60.31	25.74	31.06	28.29	62.57	39.96	15.88	14.18	50.08	22.73	20.70
Cr_2O_3	0.28	0.15	0.00	0.00	0.08	0.25	0.01	0.15	0.07	0.16	0.01	0.04	0.00	0.00	0.03	0.18	0.00
FeO*	5.88	5.73	5.17	3.66	1.32	92.02	16.30	10.38	3.78	6.86	0.58	0.69	8.39	9.12	0.63	13.45	9.14
MnO	0.11	0.14	0.10	0.10	0.05	0.02	0.31	0.12	0.03	0.13	0.01	0.01	0.07	0.08	0.01	0.04	0.16
MgO	12.70	12.75	13.50	15.97	0.04	0.00	4.19	0.00	0.16	0.00	0.06	0.07	14.60	14.82	0.48	0.00	27.53
CaO	24.55	24.83	24.30	24.79	0.02	0.00	-	23.44	23.48	23.95	0.06	0.84	12.33	12.60	11.44	23.60	0.06
Na_2O	0.00	0.15	0.15	0.05	0.00	0.00	-	0.00	0.00	0.00	0.00	7.16	2.30	2.52	1.46	0.00	0.00
K_2O	0.00	0.00	0.01	0.00	0.00	0.01	-	0.00	0.04	0.01	0.01	0.67	0.29	0.11	0.01	0.00	0.03
ZnO	-	-	-	-	-	-	19.48	-	-	-	-	-	-	-	-	-	-
Total	100.25	100.49	100.23	100.24	100.20	93.62	100.75	98.36	96.22	98.09	100.98	95.36	97.91	97.64	95.48	98.46	87.11
Atomic ratio																	
O	6	6	6	6	3	3	4	25	25	25	5	22	23	23	22	25	22
Si	1.759	1.788	1.816	1.947	0.001	0.001	0.001	6.013	5.862	5.989	1.009	5.882	6.114	6.256	4.156	6.063	5.716
Ti	0.019	0.021	0.020	0.011	0.001	0.008	0.003	0.016	0.014	0.013	0.000	0.008	0.119	0.068	0.014	0.025	0.000
Al	0.361	0.319	0.296	0.084	1.978	0.045	2.010	4.752	5.725	5.176	1.974	6.043	2.663	2.398	7.773	4.247	4.729
Cr	0.008	0.004	0.000	0.000	0.001	0.008	0.000	0.019	0.009	0.020	0.000	0.004	0.000	0.000	0.009	0.022	0.022
Fe^{3+}	0.074	0.070	0.043	0.004	0.017	1.951	-	1.223	0.445	0.801	0.012	-	0.424	0.356	-	1.605	
Fe^{2+}	0.108	0.106	0.116	0.108	-	0.975	0.385	-	-	-	-	0.074	0.575	0.739	0.074	-	1.481
Mn	0.003	0.004	0.003	0.003	0.001	0.001	0.007	0.016	0.004	0.017	0.000	0.001	0.008	0.010	0.000	0.006	0.027
Mg	0.698	0.699	0.739	0.870	0.001	0.000	0.176	0.000	0.037	0.000	0.002	0.013	3.097	3.173	0.083	0.000	7.951
Ca	0.970	0.978	0.956	0.970	0.000	0.000	-	3.934	3.935	3.983	0.002	0.115	1.880	1.938	1.660	4.008	0.011
Na	0.000	0.011	0.011	0.004	0.000	0.000	-	0.000	0.000	0.000	0.000	1.781	0.634	0.702	0.335	0.000	0.000
K	0.000	0.000	0.001	0.000	0.000	0.000	-	0.000	0.008	0.002	0.000	0.110	0.053	0.021	0.004	0.000	0.000
Zn	-	-	-	-	-	-	0.407	-	-	-	-	-	-	-	-	-	
Total	4.000	4.000	4.000	4.000	2.000	2.989	2.990	15.973	16.039	16.001	2.999	14.032	15.567	15.660	14.109	15.975	19.938

FeO*: total iron as FeO.

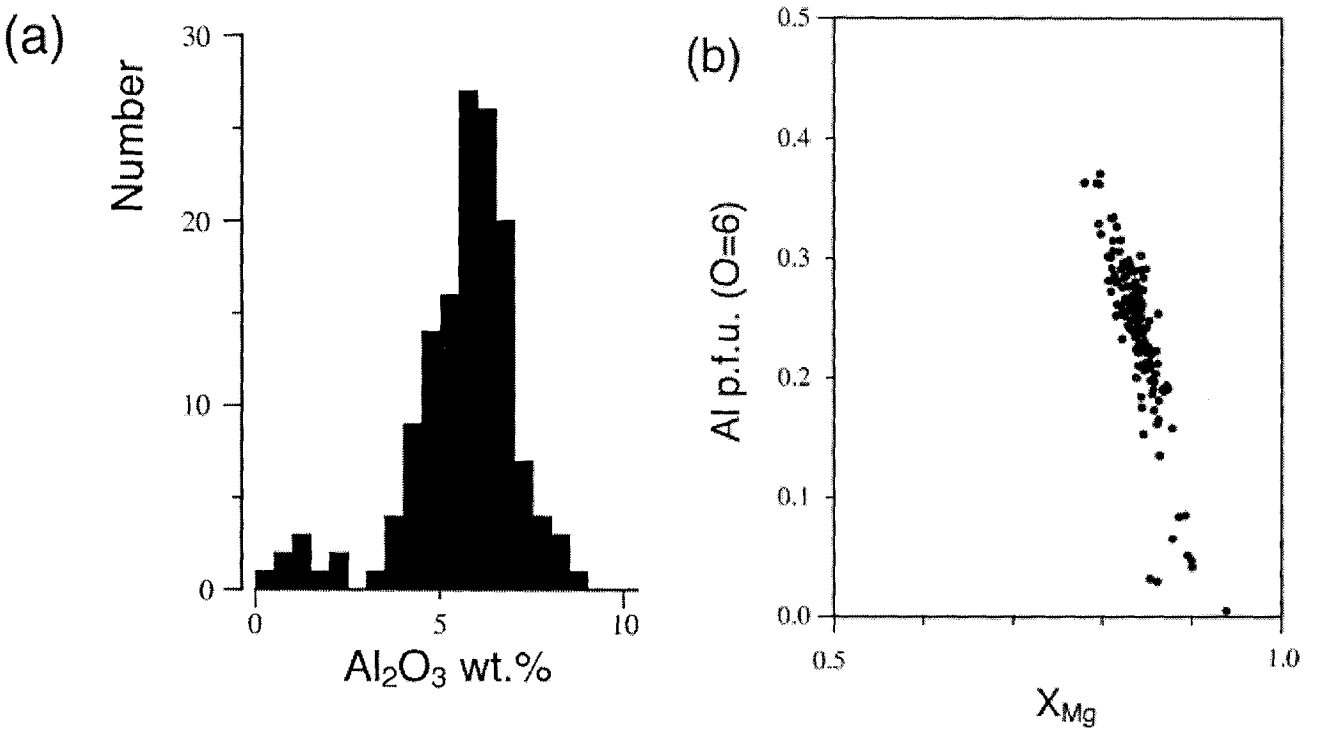

Fig. 3. Compositional variation of relict clinopyroxene in (a) Al_2O_3 (wt.%) histogram, and (b) Al p.f.u. versus X_{Mg} diagram.

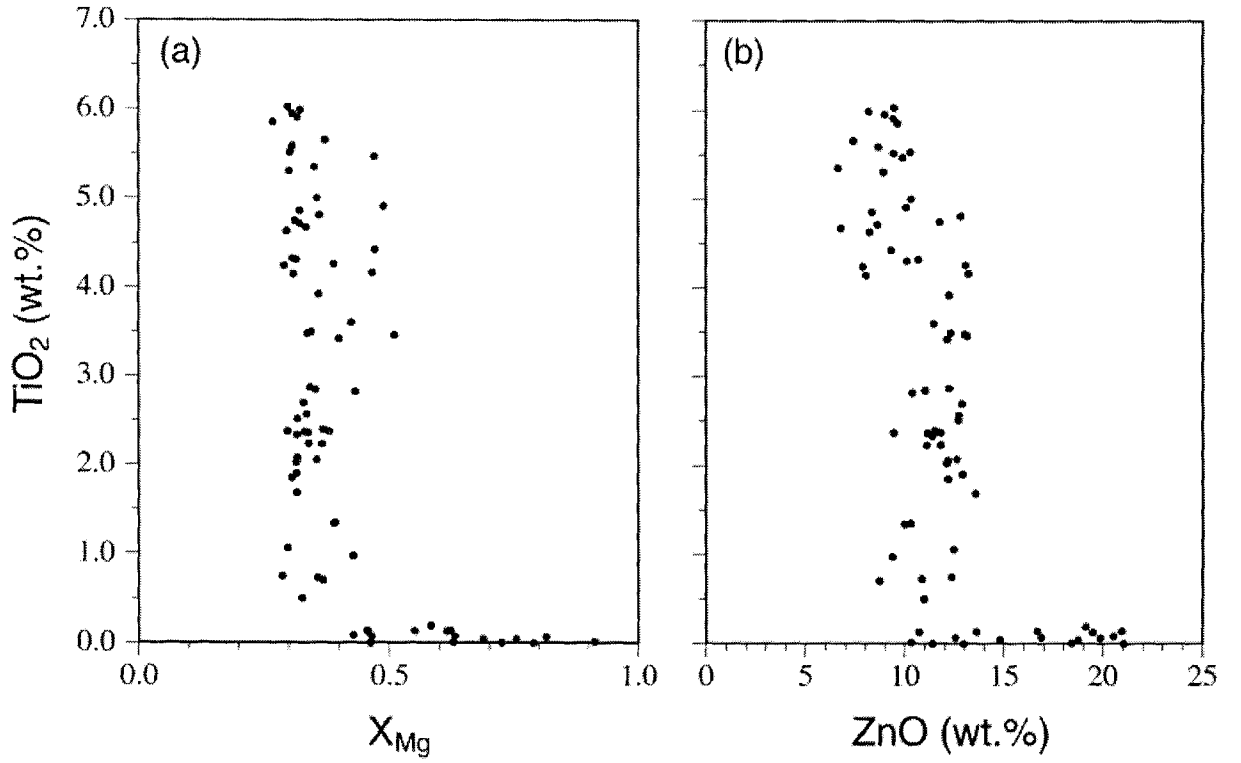

Fig. 4. Compositional variation of gahnitic spinel in the corundum-magnetite symplectite in (a) TiO_2 (wt.%) versus (a) X_{Mg} and (b) ZnO (wt.%).

the spinel pseudomorph is aluminous (Al p.f.u. = 5.6–5.9, O = 28), and its X_{Mg} ranges from 0.70 to 0.75. Chlorite in the chlorite-rich clot shows wider compositional range (Al p.f.u. = 5.0–5.9, X_{Mg} = 0.65–0.87).

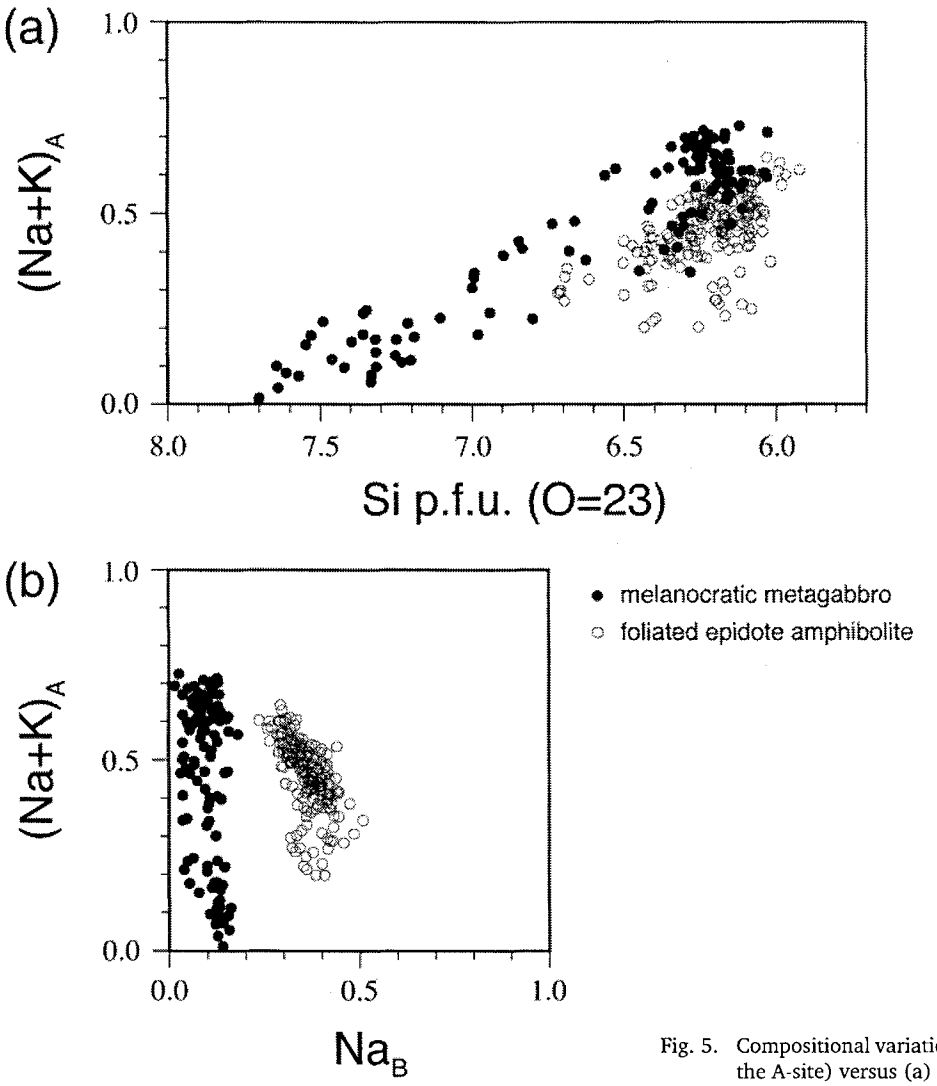

Fig. 5. Compositional variation of Ca-amphiboles in the $(Na+K)_A$ (Na+K on the A-site) versus (a) Si and (b) Na_B (Na on the B-site).

Metamorphic Evolution

Based on the observed texture, three different metamorphic stages (granulite facies stage, epidote amphibolite facies stage and retrograde stage) are defined in the melanocratic metagabbro as described below. A summary of mineral paragenesis for each stage is given in figure 6.

Granulite facies stage

The granulite facies stage is characterized by Al-rich clinopyroxene and spinel. The minerals of this stage are preserved either as relics (clinopyroxene) or as pseudomorph (spinel and plagioclase). The Al-rich clinopyroxene is common in the lower crustal basic and ultrabasic granulite with two pyroxenes+plagioclase+Al spinel assemblage (e.g., Yokoyama, 1980; Rivalenti et al., 1981; Ishiwatari, 1985a; Wilshire et al., 1991; McGuire, 1994). In our melanocratic metagabbro, the kyanite-bearing clinozoisite-rich domains that fill interstices between relict clinopyroxenes and spinel pseudomorphs are interpreted as recrystallized, originally plagioclase-rich parts. Although no relict plagioclase occurs in the melanocratic metagabbro, earlier stage plagioclase (An_{26-33}) was described as tiny inclusions in kyanite from the foliated epidote amphibolite (Tsujimori, 1999). This also supports the presence of plagioclase prior to formation of the clinozoisite+kyanite assemblage. Orthopyroxene might also have originally been present in the melanocratic metagabbro, but no evidence has so far been available. The Al-rich clinopyroxene+spinel+plagioclase± orthopyroxene (?) assemblage and absence of garnet indicate the medium-pressure granulite facies, which is bracketed by the spinel-gabbro field in the system $CaO-MgO-Al_2O_3-SiO_2$ (Gasparik, 1984; Schmädicke, 2000), suggesting the pressure around 1.0 GPa. In the

mineral \ stage	granulite	epidote amphibolite	retrograde
clinopyrxene			
spinel pseudomorph*			
Ca-amphibole			
clinozoisite (+ zoisite)			
kyanite			
paragonite			
margarite			
chlorite			
epidote			
rutile			
magnetite			

*) corundum + magnetite ± gahnite ± ilmenite

Fig. 6. Mineral parageneses for the different stages of evolution.

spinel-gabbro field, the Al content (Ca-tschermakite component) of clinopyroxene is higher than that in the olivine gabbro and garnet gabbro fields, and is strongly temperature dependent (e.g., Obata, 1976; Gasparik, 1984). The Al content (up to 8.5 wt.% Al_2O_3) in our relict clinopyroxene suggests the temperature around 800–900°C. The decomposition of spinel into corundum-magnetite symplectite will be discussed later.

Epidote amphibolite facies stage

The epidote amphibolite facies stage is represented by the clinozoisite+kyanite assemblage in the clinozoisite-rich domain. This assemblage has been reported from some highly aluminous basic and ultrabasic rocks of the high-pressure epidote amphibolite facies and the eclogite facies (e.g., Cotkin, 1988; Gil Ibarguchi et al., 1991). The clinozoisite (or zoisite)+kyanite assemblage is stable at the pressures higher than about 1.0 GPa in the system CaO-Al_2O_3-SiO_2-H_2O system (e.g., Chatterjee et al., 1984). It is noteworthy that paragonite and kyanite are in equilibrium with clinozoisite. As mentioned above, the Al-poor part of clinopyroxene is always adjacent to Ca-amphibole or clinozoisite. This may be correlated with re-equilibration during epidote amphibolite facies stage.

Retrograde stage

The retrograde stage is characterized by the breakdown of the clinozoisite+kyanite assemblage to form secondary margarite. Corundum in the corundum-magnetite symplectite is sometimes replaced by margarite. The actinolitic (or tremolitic) rim of Ca-amphibole, prismatic epidote, and chlorite are also interpreted as products of the retrograde stage. This stage represents greenschist facies overprinting after epidote amphibolite facies.

Discussions

Formation of corundum-magnetite symplectite

The corundum-magnetite intergrowth could have been produced by oxidation of hercynitic (Fe-rich) spinel. This reaction is ideally written as

hercynite ($3FeAl_2O_4$)+(O) = corundum ($3Al_2O_3$)+ magnetite (Fe_3O_4) (1).

The effect of oxygen fugacity for oxidation of hercynitic spinel is shown in figure 7. The reaction curve is located at a position between HM and QFM buffer curves at temperatures higher than about 500°C, and the decrease of activity of hercynite component shifts the reaction to higher oxygen fugacity side. It is possible that the oxidation of the original spinel occurred during the cooling

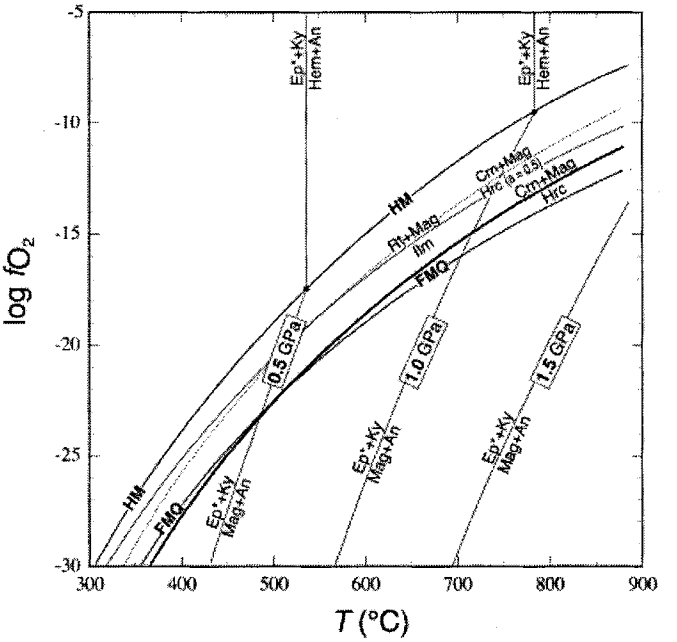

Fig. 7. The effect of oxygen fugacity for oxidation of hercynite on a log fO_2 versus T diagram. The solid lines are oxidation reaction for pure hercynite (Hrc+O_2 = Crn+Mag) and the dashed line represents an isopleth that the activity is 0.5 for hercynite. For comparison, the upper temperature limit for the assemblage epidote+kyanite at 0.5 GPa, 10 GPa, and 1.5 GPa, are also illustrated. The activity of epidote for 0.4 is used for calculations. The HM and QFM are the hematite-magnetite buffer, and the quartz-fayalite-magnetite buffer curves, respectively. Abbreviations: An = anorthite, Crn = corundum, Ep = epidote, Hem = hematite, Ilm = ilmenite, Mag = magnetite, Rt = rutile.

process through the reaction with the oxidizing fluid. In the basic to ultrabasic moderate-pressure granulite, however, Al spinel commonly bears significant Mg-spinel component as much as X_{Mg} = 0.35–0.67 (e.g., Yokoyama, 1980; Rivalenti et al., 1981; Ishiwatari, 1985a; Vysotskiy, 1994; McGuire, 1994). In contrast, our spinel pseudomorph is almost free from Mg, excepting gahnitic

spinel (X_{Mg} = 0.43–0.92) associated with the corundum-magnetite intergrowth. This indicates Mg-depletion during oxidation of original spinel. Considering the effect of Mg-spinel component expected in the original spinel, the oxidation might have taken place at a physical condition somewhere between the reaction (1) and HM buffer lines with decreasing of temperature.

Similar oxidation to produce corundum-magnetite symplectite was reported as a retrograde recrystallization of hercynitic spinel in the hercynite-quartz granulite from Namaqualand (South Africa), where the peak P–T condition of 0.65± 0.05 GPa at 800± 50°C was estimated (Waters, 1991). Spinel partly replaced by corundum-magnetite symplectite was described in meta-pegmatite of low-pressure granulite (ca. 0.32–0.34 GPa and 650–700°C) from Reynolds Range, Central Australia (Buick et al., 1998). The corundum-magnetite symplectite was documented as a prograde relic included within garnet in the pelitic granulite from the Hisøy-Torungen (South Norway) (Knudsen, 1996). In this case, the P–T condition of the symplectite formation was estimated to be about 0.36± 0.05 GPa at 800± 50°C. High-temperature condition greater than 920°C at around 0.7 GPa was inferred for the granulite facies metapelite, which bears analogous corundum-magnetite intergrowth, in a contact aureole of Eastern Ghats Belt (India) (Dasgupta et al., 1997). These analogous occurrences suggest the temperature around 700–900°C for oxidation to form corundum-magnetite symplectite in the melanocratic metagabbro from the Fuko Pass mass.

Turnock and Eugster (1962) determined the compositional limit of magnetite-hercynite solid solution in equilibrium with corundum at 0.2 GPa. They showed that Al_2O_3 content in magnetite (i.e., hercynite component) was increasing with temperature and decreasing with oxygen fugacity, but the effect of pressure had not been examined. Fe_2O_3-rich corundum (0.9–1.5 wt.%) had been synthesized at 900–1050°C and 0.90–1.57 GPa with a graphite buffer (roughly the same oxygen fugacity as the QFM buffer) in the experimental study of Shulters and Bohlen (1989), who determined the stability of hercynite+sillimanite. The high-Fe_2O_3 content of corundum in our spinel pseudomorph may also imply the high-temperature condition for the spinel oxidation.

P–T path

The granulite facies relics reported here indicate that the Fuko Pass metacumulate has experienced the granulite facies metamorphism (1.0 GPa, 800–900°C) prior to the epidote amphibolite facies metamorphism characterized by the kyanite+clinozoisite assemblage. Although the complete granulite facies assemblage is not preserved, the approximate P–T conditions of relict granulite facies assemblage may have been within the field (G) in figure 8. Hydrous mineral assemblage developed in the rock indicates the infiltration of H_2O-rich fluid after granulite facies metamorphism. The approximate P–T condition of the epidote amphibolite stage is restricted in the stability field of the clinozoisite+kyanite assemblage.

Tsujimori (1999) showed that the foliated epidote amphibolite from the Fuko Pass mass had experienced the early Paleozoic subduction metamorphism characterized by the kyanite+clinozoisite+paragonite+albite assemblage. As mentioned before, both the foliated epidote amphibolite and melanocratic metagabbro were collected from a same outcrop. Therefore, they should have recorded the same epidote amphibolite facies metamorphism. The upper temperature and pressure limits for the assemblage is restricted by the following quartz-free reactions in the system CaO-Na_2O-Al_2O_3-SiO_2-H_2O:

clinozoisite+kyanite+albite = anorthite+paragonite

paragonite = corundum+anorthite+H_2O, and

paragonite = jadeite+kyanite+H_2O (Fig. 8).

The lower pressure limits of the clinozoisite+kyanite+albite and clinozoisite+kyanite shift to the high-pressure side by the increase of Y_{Fe} in clinozoisite. Although P–T path of hydration from granulite to high-pressure epidote amphibolite is debatable, it may require tectonic burial and hydration of lower crustal granulite. We regard the P–T trajectory from the granulite facies to high-pressure epidote amphibolite facies as a pass with significant pressure increase and cooling.

In the foliated epidote amphibolite from the Fuko Pass mass, furthermore, a retrograde P–T path was estimated from the breakdown of the clinozoisite+kyanite assemblage to produce margarite with secondary plagioclase ($An_{\sim 38}$) by the decompression (Tsujimori, 1999) (Fig. 8). Although the secondary plagioclase associated with margarite have not yet been found in the melanocratic metagabbro, the melanocratic metagabbro may also have experienced the same retrograde path as the foliated epidote amphibolite.

Tectonic implications

As mentioned above, the bulk chemistry of the Fuko Pass metacumulate is consistent with the original rocks being highly fractionated troctolitic cumulate. The troctolitic to anorthositic cumulate is common in Ishiwatari's (1985b) plagioclase-type cumulates of 'non-island arc origin' ophiolites. The high-TiO_2 content (up to 0.9 wt.%) of relict clinopyroxene is also consistent with that of the plagioclase-type cumulates. In fact, high-Ti clinopyroxenes containing 0.5–1.7 wt.% TiO_2 have been

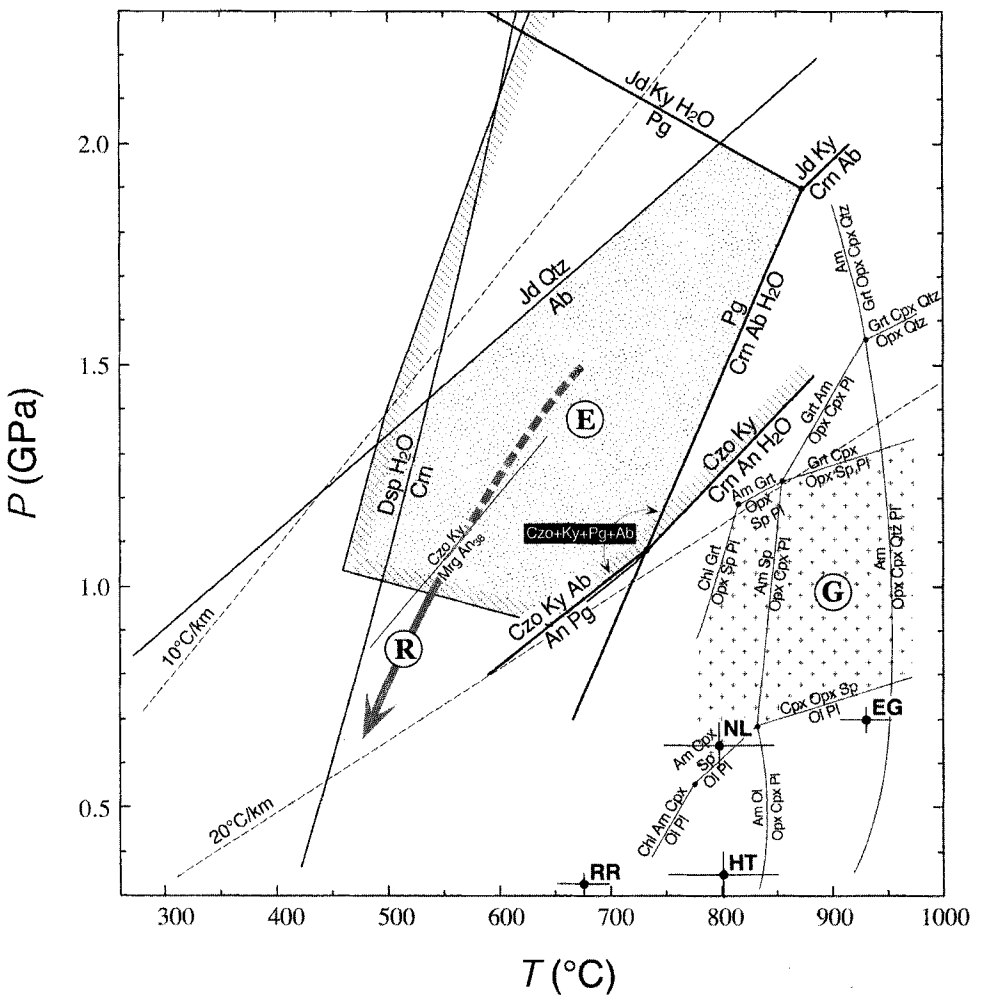

Fig. 8. P-T diagram showing the appreciate P-T condition for the relict granulite stage (G), epidote amphibolite stage (E), and the retrograde stage (R). The hatched area represents the estimated P-T field for the epidote amphibolite stage of the Fuko Pass metacumulate mass, and solid arrow shows possible retrograde path proposed by Tsujimori (1999). Solid line decorated with hatch shows that the stability field of the Czo+Ky. Bold reactions represent the quartz-free reactions to define the stability field of the Czo+Ky+Pg+Ab. The other reaction curves were computed using THERMOCALC (Powell and Holland, 1988; Powell et al., 1998) Ver. 2.7 with the HP98 dataset (Holland and Powell, 1998). The petrogenetic grids by Schmädicke (2000) are used to define a field (G). Cross bars represent the P-T ranges of granulites with corundum-magnetite symplectite in the literatures: Eastern Ghats Belt (EG), India (Dasgupta et al., 1997), Namaqualand (NL) South Africa (Waters, 1991), Hisøy-Torungen (HT), South Norway (Knudsen, 1996) and Reynolds Range (RR), Central Australia (Buick et al., 1998). Geothermal gradients of 10°C/km and 20°C/km are shown as dotted lines for reference. Abbreviations: Ab = albite, Am = amphibole, An = anorthite, Chl = chlorite, Crn = corundum, Czo = clinozoisite, Cpx = clinopyroxene, Dsp = diaspore, Grt = garnet, Jd = jadeite, Ol = olivine, Opx = orthopyroxene, Pg = paragonite, Phe = phengite, Pl = plagioclase, Qtz = quartz; Sp = spinel.

reported in the lower crustal xenoliths from the Kerguelen Plateau (Grégoire et al., 1998). The granulite facies relics and chemistry of clinopyroxene of the melanocratic metagabbros from the Fuko Pass metacumulate mass imply that the rocks constituted the lower part of thick oceanic crust. Furthermore, the high-pressure hydration posterior to the incipient granulite facies metamorphism indicates that the mass has experienced a high-P/T type metamorphism at a subduction zone.

The lower crustal basic to ultrabasic granulites, which were later recrystallized under the relatively high-pressure and medium-temperature conditions, ranging from the epidote amphibolite facies to the eclogite facies, occur sometimes in the collisional orogenic belts (e.g., Western Gneiss Region: Cotkin, 1997; Eastern Central Alps: Münttener et al., 2000), but they are rare in the Circum-Pacific orogenic belts. The relict granulite facies assemblage has only been known in the eclogitic gneiss - peridotite complex (eastern Iratsu and Nikubuchi masses) of the Sambagawa metamorphic belt, Central Shikoku, Japan (e.g., Yokoyama, 1980; Goto and Banno, 1990; Tanaka, 2001). The Nikubuchi mass of the Sambagawa belt experienced the granulite facies metamorphism prior to the high-pressure metamorphism characterized by the

kyanite+zoisite assemblage (Yokoyama, 1980). The metamorphic evolution of the Fuko Pass mass is similar to that of the Nikubuchi mass, and is clearly different from those of lower crustal granulites in some Circum-Pacific ophiolites, which have been emplaced without experiencing subduction. Cloos (1993) argued that the thick oceanic crust is buoyant enough to resist subduction, and cause collisional orogenesis at subduction zones. Saunders et al. (1996) mentioned that the introduction of H_2O-rich fluid at the lower part of unusually thick oceanic crust allows transformation of lower crustal granulite to eclogite during collisional orogenesis. The granulite facies relics in the Fuko Pass metacumulate mass may be another rare example showing the subduction of thick oceanic crust. The lower crustal granulites that experienced high-P/T type metamorphism in Circum-Pacific orogens may show an evidence of the subduction or collisional crustal thickening of the thick oceanic crust.

Acknowledgment

This research was supported financially in part by the JSPS research fellowship for young scientists of the first author. We thank M. Arima and T. Hirajima for their careful and insightful reviews. We also extend our thanks to T. Itaya who provided the opportunity for publication.

References

Arai, S. (1975) Contact metamorphosed dunite-harzburgite complex in the Chugoku district, western Japan. Contrib. Mineral. Petrol., v. 52, pp. 1-16.

Arai, S. (1980) Dunite-harzburgite-chromitite complexes as refractory residue in the Sangun-Yamaguchi Zone, western Japan. J. Petrol., v. 21, pp. 141-165.

Buick, I.S., Cartwright, I. and Harley, S.L. (1998) The retrograde P–T–t oath for low-pressure granulites from the Reynolds Range, Central Australia: petrological constraints and implications for low-P/high-T metamorphism. J. Metam. Geol., v. 16, pp. 511-529.

Chatterjee, N.D. (1976) Margarite stability and compatibility relations in the system CaO-Al_2O_3-SiO_2-H_2O as a pressure-temperature indicator. Amer. Mineral., v. 61, pp. 699-709.

Chatterjee, N.D., Johannes, W. and Leistner, H. (1984) The system CaO-Al_2O_3-SiO_2-H_2O: new phase equilibria data, some calculated phase relations, and their petrological applications. Contrib. Mineral. Petrol., v. 88, pp. 1-13.

Cloos, M. (1993) Lithospheric buoyancy and collisional orogenesis: subduction of oceanic plateaus, continental margins, island arcs, spreading ridges, and seamounts. Geol. Soc. Amer. Bull., v. 105, pp. 715-737.

Cotkin, S.J. (1997) Igneous and metamorphic petrology of the eclogitic Seljeneset meta-anorthosite and related jotunites, Western Gneiss Region, Norway. Lithos, v. 40, pp. 1-30.

Cotkin, S.J., Valley, J.W. and Essene, E.J. (1988) Petrology of a margarite-bearing meta-anorthite from Seljeneset, Nordfjord, western Norway: implications for the P–T history of the Western Gneiss Region during Caledonian uplift. Lithos, v. 21, pp. 117-128.

Dasgupta, S., Ehl, J., Raith, M.M., Sengupta, P. and Sengupta, P. (1997) Mid-crustal contact metamorphism around the Chimakurthy mafic-ultramafic complex, Eastern Ghats Belt, India. Contrib. Mineral. Petrol., v. 129, pp. 182-197.

DeBari, S.M. and Coleman, R.G. (1989) Examination of the deep levels of an island arc: evidence from the Tonsina ultramafic-mafic assemblage, Tonsina, Alaska. J. Geophys. Res., v. 94, pp. 4373-4391.

Francis, D.M. (1976) Corona-bearing pyroxene granulite xenoliths and the lower crust beneath Nunivak Island, Alaska. Can. Mineral., v. 14, pp. 291-298.

Gasparik, T. (1984) Two-pyroxenes thermobarometry with new experimental data in the system CaO-MgO-Al_2O_3-SiO_2. Contrib. Mineral. Petrol., v. 87, pp. 87-97.

Gil Ibarguchi, J.I., Mendia, M. and Girardeau, J. (1991) Mg- and Cr-rich staurolite and Cr-rich kyanite in high-pressure ultrabasic rocks (Cabo Ortegal, northwestern Spain). Amer. Mineral., v. 76, pp. 501-511.

Goto, A. and Banno, S. (1990) Hydration of basic granulite to garnet-epidote amphibolite in the Sambagawa metamorphic belt, Central Shikoku, Japan. Chem. Geol., v. 85, pp. 247-263.

Grégoire, M., Cottin, J.Y., Giret, A., Mattielli, N. and Weis, D. (1998) The meta-igneous granulite xenoliths from Kerguelen Archipelago: evidence of a continent nucleation in an oceanic setting. Contrib. Mineral. Petrol., v. 133, pp. 259-283.

Grégoire, M., Mattielli, N., Nicollet, C., Cottin, J.Y., Leyrit, H., Weis, D., Shimizu, N. and Giret, A. (1994) Oceanic granulite from the Kerguelen Archipelago. Nature, v. 367, pp. 360-363.

Hayasaka, Y., Sugimoto, T. and Kano, T. (1995) Ophiolitic complex and metamorphic rocks in the Niimi-Katsuyama area, Okayama Prefecture. Excursion Guidebook of 102nd Annual Meeting of the Geol. Soc. Japan, pp. 71-87 (in Japanese).

Holland, T.J.B. and Powell, R. (1998) An internally consistent thermodynamic data set for phases of petrological interest. J. Metam. Geol., v. 19, pp. 309-343.

Ishiga, H. and Suzuki, S. (1988) Late Paleozoic radiolarian assemblages from the Shimomidani Formation in Akiyoshi terrane, southwest Japan. J. Geol. Soc. Japan, v. 94, pp. 493-499.

Ishiwatari, A. (1985a) Granulite-facies metacumulates of the Yakuno ophiolite, Japan: evidence for unusually thick oceanic crust. J. Petrol., v. 26, pp. 1-30.

Ishiwatari, A. (1985b) Igneous petrogenesis of the Yakuno ophiolite (Japan) in the context of the diversity of ophiolites. Contrib. Mineral. Petrol., v. 89, pp. 155-167.

Ishiwatari, A. (1991) Time-space distribution and petrologic diversity of Japanese ophiolite. In: Peters, Tj. et al. (Eds.), 'Ophiolite genesis and evolution of the oceanic lithosphere', pp. 723-743.

Isozaki, Y. (1996) Anatomy and genesis of a subduction-related orogen: a new view of geotectonic subdivision and evolution of the Japanese Island. The Island Arc, v. 5, pp. 289-320.

Knudsen, T.L. (1996) Petrology and geothermobarometry of granulite facies metapelites from the Hisøy-Tougen area, South Norway: new data on the Sveconorvegian P–T–t path of the Bamble sector. J. Metam. Geol., v. 14, pp. 267-287.

Kuroda, Y., Kurokawa, K., Uruno, K., Kinugawa, T., Kano, H. and Yamada, T. (1976) Staurolite and kyanite from epidote-hornblende rocks in the Oeyama (Komori) ultramafic mass, Kyoto Prefecture, Japan. Earth Sci. (Chikyu Kagaku), v. 30, pp. 331-333.

Kurokawa, K. (1975) Discovery of kyanite from epidote-amphibolite in the Oeyama ultramafic mass, Inner Zone of southwestern Japan. J. Geol. Soc. Japan, v. 81, pp. 273-274.

Kurokawa, K. (1985) Petrology of the Oeyama ophiolitic complex in the Inner Zone of southwest Japan. Science Report of Niigata University (Series E), v. 6, pp. 37-113.

Maruyama, S. (1997) Pacific-type orogeny revisited: Miyashiro-type orogeny proposed. The Island Arc, v. 6, pp. 91-120.

Matsumoto, I., Arai, S. and Yamauchi, H. (1997) High-Al podiform chromitites in dunite-harzburgite complexes of the Sangun zone, Central Chugoku district, southwest Japan. J. Asian Earth Sci., v. 15, pp. 295-302.

McGuire, A.V. (1994) Southern basin and range province crust-mantle boundary: evidence from gabbroic xenoliths, Wikieup, Arizona. J. Geophys. Res., v. 99, pp. 24263-24273.

Müntener, O., Hermann, J. and Trommsdorff, V. (2000) Cooling history and exhumation of lower-crustal granulite and upper mantle (Malenco, eastern Central Alps). J. Petrol., v. 41, pp. 175-200.

Nishimura, Y. and Shibata, K. (1989) Modes of occurrence and K–Ar ages of metagabbroic rocks in the "Sangun metamorphic belt", southwest Japan. Geol. Soc. Japan, Mem. No. 33, pp. 343-357 (in Japanese with English abstract).

Obata, M. (1976) The solubility of Al_2O_3 in orthopyroxenes in spinel and plagioclase peridotites and spinel pyroxenite. Amer. Mineral., v. 61, pp. 804-816.

Powell, R. and Holland, T.J.B. (1988) An internally consistent thermodynamic dataset with uncertainties and correlations: 3. Applications to geobarometry, worked examples and a computer program. J. Metam. Geol., v. 6, pp. 173-204.

Powell, R., Holland, T.J.B. and Worley, B. (1998) Calculating phase diagrams involving solid solutions via non-linear equations, with examples using THERMOCALC. J. Metam. Geol., v. 16, pp. 577-588.

Rivalenti, G., Garuti, G., Rossi, A., Siena, F. and Sinigoi, S. (1981) Existence of different peridotite types and of a layered igneous complex in the Ivrea Zone of the western Alps. J. Petrol., v. 22, pp. 127-153.

Saunders, A.D., Tarney, J., Kerr, A.C. and Kent, R.W. (1996) The formation and face of large oceanic igneous provinces. Lithos, v. 37, pp. 81-95.

Schmädicker, E. (2000) Phase relations in peridotitic and pyroxenetic rocks in the model systems CMASH and NCMASH. J. Petrol., v. 41, pp. 69-86.

Shulters, J.C. and Bohlen, S.R. (1989) The stability of hercynite and hercynite-gahnite spinel in corundum- or quartz-bearing assemblage. J. Petrol., v. 30, pp. 1017-1031.

Takahashi, E. (1978) Petrologic model of the crust and upper mantle of the Japanese island arcs. Volc. Bull., v. 414, pp. 529-546.

Tanaka, C. (2001) The reaction process from granulite to eclogite in the eastern Iratsu epidote amphibolite mass in the Sambagawa belt, Central Shikoku, Japan. Abstract of 6th International Eclogite Conference, Niihama, Japan. p. 161.

Tsujimori, T. (1999) Petrogenesis of the Fuko Pass high-pressure metacumulate from the Oeyama peridotite body, southwestern Japan: evidence for early Paleozoic subduction metamorphism. Geol. Soc. Japan, Mem. No. 52, pp. 287-302.

Tsujimori, T. and Itaya, T. (1999) Blueschist-facies metamorphism during Paleozoic orogeny in southwestern Japan: phengite K–Ar ages of blueschist-facies tectonic blocks in a serpentinite melange beneath early Paleozoic Oeyama ophiolite. The Island Arc, v. 8, pp. 190-205.

Tsujimori, T., Nishina, K., Ishiwatari, A. and Itaya, T. (2000) 403–443 Ma kyanite-bearing epidote amphibolite from the Fuko Pass metacumulate in Oeyama, the Inner Zone of southwestern Japan. J. Geol. Soc. Japan, v. 106, pp. 646-649 (in Japanese with English abstract).

Turnock, A.C. and Eugster, H.P. (1962) Fe-Al oxides: phase relationships below 1,000°C. J. Petrol., v. 3, pp. 533-565.

Uda, S. (1984) The contact metamorphism of the Oeyama ultrabasic mass and the genesis of the "cleavable olivine". J. Geol. Soc. Japan, v. 90, pp. 393-410 (in Japanese with English abstract).

Vysotskiy, S.V. (1994) High and low pressure cumulates of Paleozoic ophiolites in Primorye, eastern Russia. In: Ishiwatari et al. (Eds.), Circum-Pacific Ophiolites (Proceedings of the 29th IGC Ophiolite Symp.). VSP Publishers, Netherlands. pp. 145-162.

Waters, D.J. (1991) Hercynite-quartz granulites: phase relations, and implications for crustal processes. Eur. J. Mineral., v. 3, pp. 369-386.

White, R.S., NcKenzie, D. and O'Nions, R.K. (1992) Oceanic crustal thickness from seismic measurements and rare earth element inversions. J. Geophys. Res., v. 97, pp. 19683-19715.

Wilshire, H.G., McGuire, A.V., Noller, J.S. and Turrin, B.D. (1991) Petrology of lower crustal and upper mantle xenoliths from the Chima Volcanic Field, California. J. Petrol., v. 32, pp. 169-200.

Yokoyama, K. (1980) Nikubuchi peridotite body in the Sanbagawa metamorphic belt; thermal history of the 'Al-pyroxene-rich suite' peridotite body in high pressure metamorphic terrain. Contrib. Mineral. Petrol., v. 73, pp. 1-13.